ECMWF Feature article

from Newsletter Number 114 – Winter 2007/08

METEOROLOGY

Advances in simulating atmospheric variability with IFS cycle 32r3

www.ecmwf.int/en/about/news-centre/media-resources

doi:10.21957/33vbh2pla1

This article appeared in the Meteorology section of ECMWF Newsletter No. 114 – Winter 2007/08, pp. 29-38.

Advances in simulating atmospheric variability with IFS cycle 32r3

Peter Bechtold, Martin Köhler, Thomas Jung,
Martin Leutbecher, Mark Rodwell, Frederic Vitart

Forecasting the state of the atmosphere involves the prediction of a slowly evolving mean equilibrium state (also referred to as the climate) and the temporal and spatial variations around this state. Predicting the amplitude and phase of the planetary, synoptic and mesoscale perturbations is not an easy task. This is especially so in the tropics where with decreasing latitude the radius of influence (also called Rossby radius of deformation) over which a given perturbation impacts on the background flow extends to infinity. Consequently the perturbations can actually circle the entire tropical belt.

Issues related to atmospheric variability as predicted using ECMWF's Integrated Forecast System (IFS) particularly concern the following.

- A decrease in amplitude of tropical synoptic and planetary-scale activity within the first ten days of the forecast.
- A slight underestimation of mid-latitude synoptic activity in the medium range.
- A lack of growth of the ensemble spread in mid-latitudes in the Ensemble Prediction System (EPS) that is compensated by choosing large initial perturbations.
- An underestimation in the total amount of precipitation and the amplitude of the annual cycle over the tropical continents.

Some of these issues are not specific to the IFS, but are shared by many global atmospheric modelling systems.

The relative activity of a model can be defined as the standard deviation of forecast anomalies divided by the standard deviation of observed (i.e. analysed) anomalies from the ERA-40 climatology. Figure 1 shows the relative activity as a function of forecast lead time for forecasts with model cycle 32r2 (hereafter Cy32r2) that was operational between 5 June 2007 and 6 November 2007, and cycle 32r3 (Cy32r3) that became operational on 6 November 2007 and which is the topic of this article. Relative activity is shown for 850 hPa temperatures in the northern and southern hemispheres (poleward of 20°), and for 925 hPa temperatures in the tropics. The 850 hPa temperature variations in mid-latitudes are a good measure of cold and warm advection associated with synoptic systems, whereas tropical temperatures variations at the 925 hPa level are representative of the low-level convergent/divergent circulations.

Figure 1 indicates that Cy32r2 slightly underestimates mid-latitude atmospheric activity, but more importantly underestimates activity in the tropics. This problem was also present in all previous cycles. In contrast, in Cy32r3 model activity is close to the climatology within the first ten days in both the mid-latitude and tropical regions. Indeed the dots show that the activity is significantly better compared to Cy32r2 at the 95% confidence level. The higher, but more realistic level of atmospheric activity has been achieved without compromising classical deterministic forecast scores.

In the rest of this article we consider the main features introduced with Cy32r3 and their impact on the model climate and deterministic forecasts. We also discuss the consequences of the model changes for the EPS and the monthly forecasts.

Features of Cy32r3

The two main physical processes that lead to the generation of kinetic energy in the atmosphere are radiative cooling/heating and convective heating, with the differential radiation being the actual driving force of the general circulation. On sufficiently large space and time scales the two processes are in quasi-equilibrium above the boundary layer. Inside the boundary layer, it is the turbulent diffusion that regulates the exchanges of momentum and heat between the surface and the atmosphere, and the dissipation of kinetic energy. Therefore, from a physical point of view, one would suspect one of these processes as being responsible for the lack of model activity. Recently, the radiation scheme received a substantial upgrade with a new shortwave code and the introduction of McICA (Monte Carlo Independent Column Approximation) (*Morcrette et al.,* 2007), so that the focus is now on convection and vertical diffusion.

 doi:10.21957/33vbh2pla1

However, there exists another source of kinetic energy dissipation in the model. This is the numerical diffusion that is inherent to the interpolations in the semi-Lagrangian advection scheme, but this source of dissipation is not affected by the changes associated with Cy32r3.

Before Cy32r3 the formulation of deep convection imposed a strong coupling between the convection and the large-scale dynamics through an entrainment formulation based on the large-scale moisture convergence. This, together with an iterative procedure, leads to a nonlinear feedback between the large-scale flow and convection that is difficult to control. Therefore, it was decided to remove any imposed large-scale control of the convection through the ω field (where $\omega = dp/dt$) or the moisture convergence, and to let the model find its own equilibrium. As a first step the convection scheme has been rendered quasi-linear which facilitates the optimisation of parameters. The entrainment is set proportional to the relative humidity of the environment based on the observations showing that convective cloud development is controlled by mid-tropospheric relative humidity. Furthermore the entrainment is scaled with a vertical function decreasing exponentially with height thereby mimicking an ensemble of clouds. The convective adjustment time is no longer a constant varying with model resolution (720 s at T799, and 3600 s at T159). Instead the adjustment time is a quantity equivalent to the estimated convective turnover time scale with a weak resolution dependency of a factor of two between model resolutions of T799 and T159. Finally, rain evaporation below convective clouds is set to occur with environmental relative humidities of less than 0.9 (0.7) over water (land). Different values are used over land and water in order to account for differences in the horizontal variability of the water vapour field.

Furthermore it has been realised for some time that for both stably stratified boundary layers and outside the boundary layer the model turbulent mixing, which is intended to reduce static and shear instabilities, is too strong. The consequence is that stratocumulus layers tend to be eroded, and the vertical shear of the wind is reduced. However, it turns out that stronger vertical diffusion is beneficial for deterministic forecast scores. Therefore, as a pragmatic step, it was decided to interpolate the diffusion coefficients between the former *Louis et al.* (1982) formulation in the surface layer and the formulation given by the Monin-Obukhov theory higher in the free troposphere.

Cy32r3 also contains two other major changes.

- A change in the soil hydrology scheme including a soil texture map and a new set of hydraulic properties for unsaturated soils, as well as a sub-grid surface runoff.
- A new bias correction scheme for radiosonde temperature and humidity data as a function of solar elevation and radiosonde type.

These changes have a beneficial impact on soil moisture and surface runoff. They also lead to a slightly moister analysis in the free atmosphere that more closely fits the observations.

In addition Cy32r3 includes changes in the assimilation and observing system. These concern an increase in the number of radio occultation data from COSMIC and use of additional sources of satellite data (see Table 1).

Changes to the IFS, particularly to the physical and numerical aspects, require thorough testing. It is impossible to cover all of them here, but some key diagnostics of the model climate and the quality and activity of the forecasts will now be discussed.

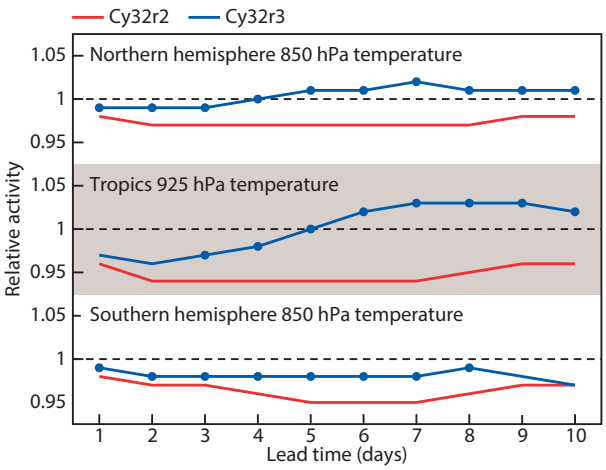

Figure 1 Relative activity in Cy32r2 and Cy32r3 as a function of forecast lead time for 850 hPa temperatures in the northern and southern hemispheres, and tropical temperatures at 925 hPa. The relative activity is defined as the ratio between the standard deviation of forecast anomalies and the standard deviation of anomalies from an ERA-40 based climatology. The blue dots denote improvements that are significant at the 95% confidence level.

Instrument	Platform
AMSR-E (Advanced Microwave Scanning Radiometer – Earth Observing System	Aqua
(SSMIS) Special Sensor Microwave Imager/Sounder	Defense Meteorological Satellite Program (DMSP)
TMI (TRMM Microwave Instrument)	Tropical Rainfall Measuring Mission
SBUV (Solar Backscatter Ultraviolet)	NOOA-17/NOAA-18
OMI (Ozone Monitoring Instrument)	Aura

Table 1 Additional sources of satellite information used in Cy32r3.

Model climate

Figure 2 compares the precipitation average from the Global Precipitation Climatology Project (GPCP, a merger of raingauge data and satellite-derived rainrates) for the December to March period with the values obtained from long integrations at resolution T159L91 for Cy31r1, Cy32r2, and Cy32r3.

- Cy31r1 has been operational between 12 September 2006 and 5 June 2007; it is also the cycle used in the Interim Reanalysis and the current seasonal forecasting system known as System 3. This cycle (and previous cycles) underestimates precipitation over the tropical continents, but overestimates precipitation over the Pacific Inter Tropical Convergence Zone (ITCZ) and the southern Indian Ocean.
- Cy32r2 with the revised radiation scheme reduces the precipitation biases, especially the convective rainfall over the tropical continents, due to stronger cloud-radiative feedback and a better description of surface shortwave heating.
- With Cy32r3 the overall rainfall distribution is further improved everywhere, including a better land sea contrast, apart from an overestimation of convective precipitation in the West Pacific. The global average precipitation rate is reduced from 3.0 to 2.9 mm/day (which is more in line with observational estimates). Also the tropical troposphere becomes significantly moister between 850 and 600 hPa (not shown).

The rainfall changes in Cy32r3 not only reflect a local effect due to the changes in convection, but also reflect changes in the large-scale circulation and the transport of moisture from the subtropics to tropical regions. Finally, take a closer look at the precipitation rates averaged over the Amazon basin and parts of the Andes (Figure 3). It is noticeable that compared to a special set of raingauge data (*Betts et al.,* 2005) Cy32r3 also improves the amplitude of the annual cycle of rainfall which has been rather flat in previous IFS cycles.

The tropical activity in the long integrations is effectively evaluated with so called wavenumber-frequency diagrams for either Outgoing Longwave Radiation (OLR), 850 hPa winds or 200 hPa velocity potential. Theory (*Gill,* 1980) says that an equatorial local heat source generates, amongst others, westward moving Rossby waves with phase speeds around 5 ms^{-1}, and eastward moving Kelvin waves with phase speeds of 15–20 ms^{-1}.

Figure 4 compares the wavenumber-frequency spectra of the predicted OLR averaged over the latitude band 10°S–10°N to spectra of the OLR observed by NOAA satellites. Notice the relative lack of power in the easterly modes (Kelvin waves) in Cy31r1 and Cy32r2. However, Cy32r3 realistically represents both Rossby and Kelvin mode activity, but now somewhat overestimates the power in the low-frequency low-wavenumber range. The dominant mode in the OLR spectrum within the positive wavenumber 1–2 band and frequency range of 20–60 days (0.05–0.016 cycles per day in Figure 4) is a signature of the Madden-Julian Oscillation (MJO). The increased wave activity in Cy32r3 also has a beneficial impact on temperatures and winds in the stratosphere and mesosphere as Rossby and Kelvin waves propagate vertically through the atmosphere. However, the increased wave activity (and associated momentum transfer during wave breaking events) is not sufficient to produce the observed Quasi-Biannual Oscillations (QBO) in the modelled stratospheric zonal winds in the tropics.

doi:10.21957/33vbh2pla1

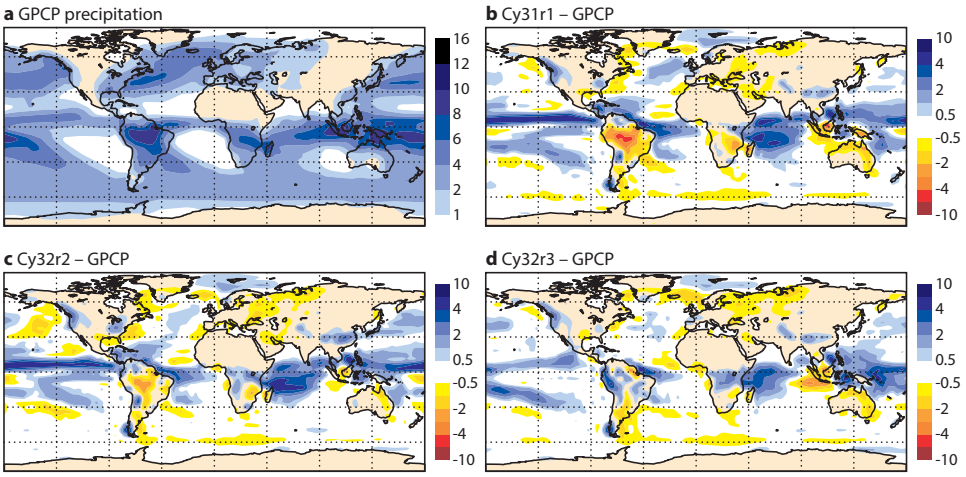

Figure 2 (a) Average precipitation rate (mm/day) for December, January and February 1990-2005 from GPCP. (b) Difference between the seasonal type integration at resolution T159 with Cy31r1 and GPCP. (c) and (d) As (b) but for Cy32r2 and Cy32r3.

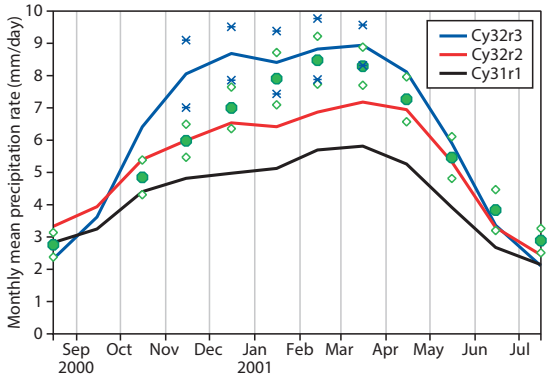

Figure 3 Annual cycle of monthly mean precipitation rates (mm/day) for Amazonia obtained from a one-year integration of a four-member T159 ensemble with Cy31r1 (black), Cy32r2 (red) and Cy32r3 (blue). The raingauge observations are denoted by the green dots and the standard deviations of monthly mean precipitation rates for the observations and Cy32r3 are denoted by green diamonds and blue crosses, respectively.

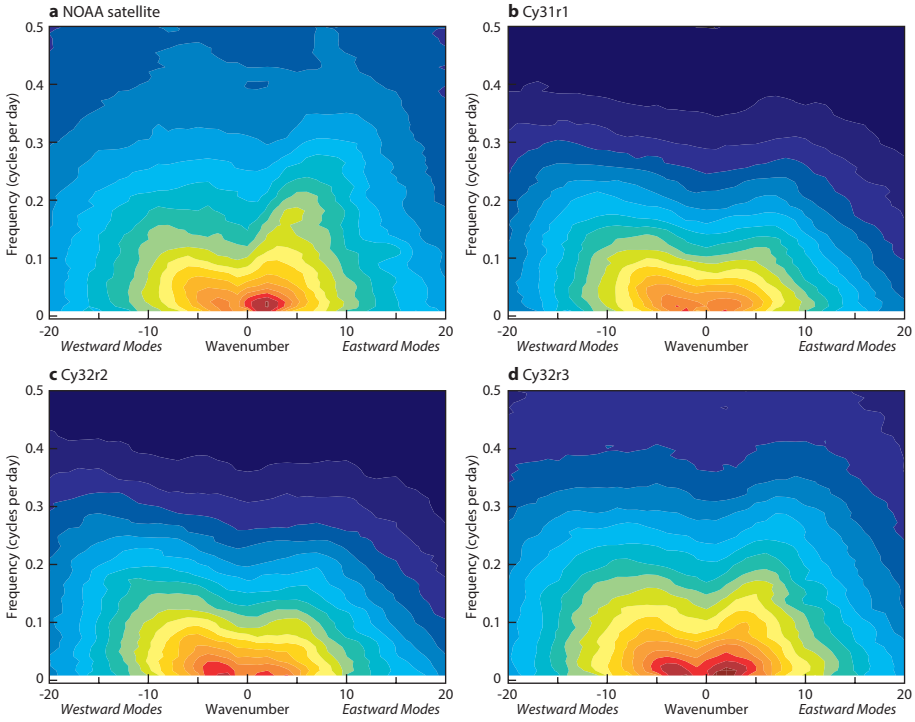

Figure 4 Power in the frequency (cycles per day) and wavenumber space for the Outgoing Longwave Radiation (OLR) in the 10°S–10°N tropical region from (a) NOAA satellite observations. (b), (c), (d) The corresponding results to (a) but for 15 winter runs (1990–2005) with Cy31r1, Cy32r2 and Cy32r3.

Deterministic forecasts

Cy32r3 has been tested in the full T799 (25 km) resolution analysis/forecast cycle for ten months from January to October 2007. Figure 5 summarizes the forecast performance of all available 00 and 12 UTC forecasts using the anomaly correlations (i.e. correlation of forecast anomalies with analysis anomalies) for the 1000 and 500 hPa geopotentials in the northern and southern hemispheres at resolution T63 (300 km) based on an ERA-40 climate. In the southern hemisphere Cy32r3 improves over Cy32r2 at all lead times. As indicated by the dots in Figure 5 these improvements are statistically significant. In the northern hemisphere the improvements are smaller and only statistically significant during the first five days. In spite of higher model activity the deterministic scores are neutral or even improved. In addition Figure 1 gives an indication of a slight over-activity in Cy32r3 in the northern hemisphere after day 5 which seems to compromise somewhat the scores in the medium range.

A comparison with surface synoptic data over Europe is given in Figure 6 for precipitation, two-metre temperature, cloud cover and ten-metre wind direction.

- The precipitation between the two cycles shows a small but significant improvement in the short-range precipitation forecasts (Figure 6(a)).
- The two-metre temperature warm bias over Europe during summer is reduced in Cy32r3, adding a cooling of 0.3 K near the surface (Figure 6(b)). This cooling is associated with a 1–2% increase in cloud cover, particularly due to shallow clouds (Figure 6(c)).
- The bias in ten-metre wind direction is also reduced by a few degrees, and now remains nearly constant with forecast lead time (Figure 6(d)). The wind direction bias actually corresponds to an underestimation of the wind turning (veering) with height, a problem that is present in many models.

The near-surface improvements are a combined effect of the revised shallow convection, the reduction in turbulent diffusion, and the better description of the soil moisture.

Since August 2005 the IFS has produced forecast-generated satellite images. These correspond to brightness temperatures (BTs) computed from the RTTOV (Radiative Transfer model for TOVS, ATOVS and Other Vertical sounders) in the 10.8 μm infrared band and the 6.2 μm water vapour band that can be directly compared to observed BTs from Meteosat 8 and Meteosat 9. As the infrared BTs have values that are very close to the actual cloud top temperatures, the synthetic images are an excellent tool for indirectly verifying the model clouds (cloud cover and condensate content) and the synoptic and convective activity associated with cloud systems.

Figure 7(a) shows the infrared satellite image from Meteosat 9 for 1 July 2007 for large parts of Europe and North Africa, with the corresponding six-hour forecast images with Cy32r2 and Cy32r3 given in Figures 7(b) and 7(c). Generally the model gives a good representation of the mid-latitude synoptic cloud systems, but has more difficulty with tropical convection. It seems, however, that Cy32r3 reproduces more realistic tropical convection associated with the African Easterly Waves between the equator and 5°N (two waves are apparent in Figure 7).

As a quantitative verification, time series from 15 June to 14 July 2007 of spatial correlations and mean errors between daily 6–24 hours forecast and observed infrared BTs are plotted in Figure 8. The errors exhibit a diurnal cycle with the largest positive biases and lowest correlations occurring during night. This indicates that the forecasts have difficulty in producing long-lived convective systems that extend into the night. With Cy32r2 the average spatial correlation between observed and forecast BTs is about 0.5. Cy32r3 slightly improves this correlation, and in particular improves the warm bias in the forecast which becomes smaller than 1 K. The improvement in Cy32r3 can be linked to the more intense continental convection and larger upper-level convective detrainment, producing more and colder anvil clouds, and to an improved analysis using the new radiosonde bias correction scheme. Applying the same type of verification for Europe (not shown), the two cycles produce nearly identical results, but correlations between observed and forecast BTs are much higher with values around 0.8.

doi:10.21957/33vbh2pla1

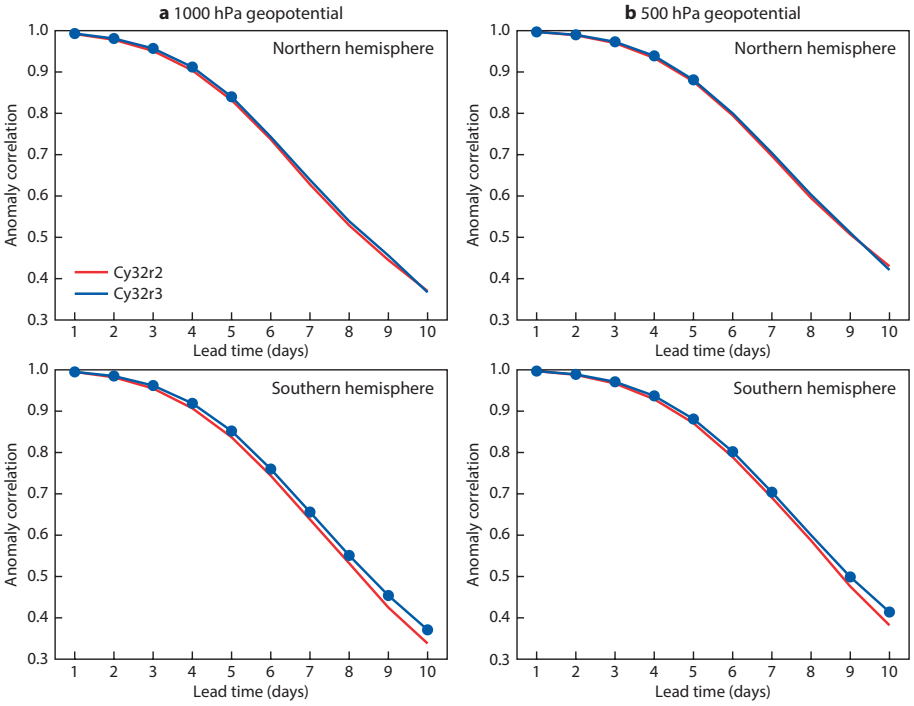

Figure 5 Average anomaly correlations for Cy32r2 and Cy32r3 as a function of forecast lead time for the northern hemisphere (20°N–90°N, top panel) and southern hemisphere (20°S–90°S, bottom panel) for (a) 1000 hPa geopotential and (b) 500 hPa geopotential for January to October 2007. The blue dots denote improvements that are significant at the 95% confidence level.

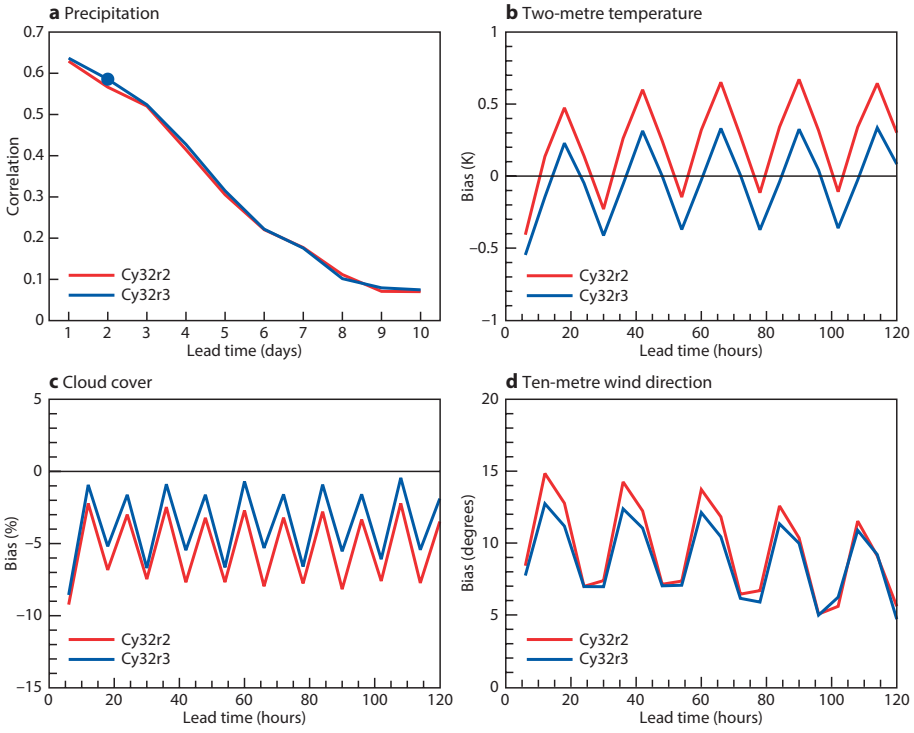

Figure 6 Evaluation of the high-resolution deterministic forecasts with Cy32r2 and Cy32r3 against surface synoptic observations for Europe as a function of forecast lead time: (a) correlation of precipitation, (b) bias of two-metre temperature, (c) bias of cloud cover and (d) bias of ten-metre wind direction. Data is for summer 2007.

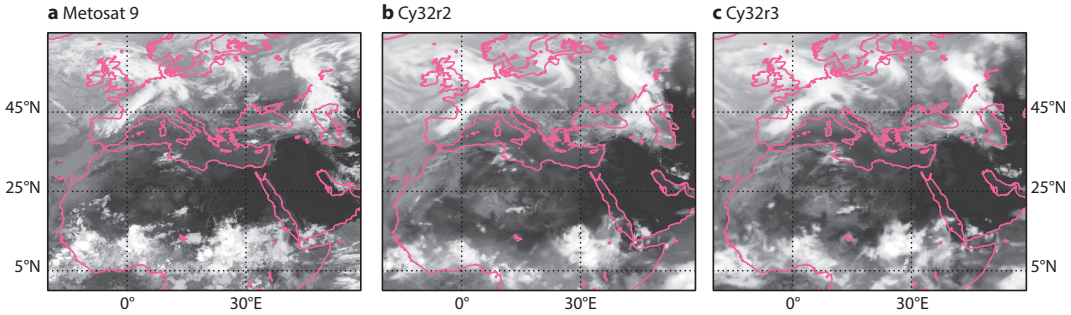

Figure 7 (a) Observed infrared 10.8 μm brightness temperatures (BTs) from Meteosat 9 for 06 UTC on 1 July 2007. (b), (c) The corresponding RTTOV generated BTs from six-hour forecasts with Cy32r2 and Cy32r3.

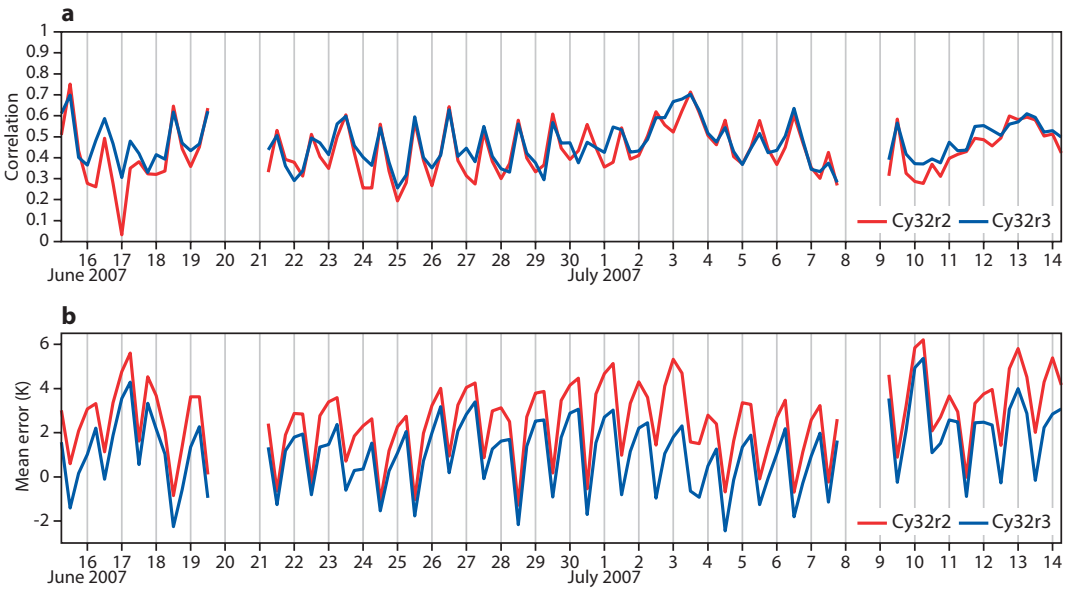

Figure 8 Time series from 15 June to 14 July 2007 of (a) correlation and (b) mean error of forecast synthetic 10.8 μm BTs obtained with Cy32r2 and Cy32r3 against Meteosat 9 observations. Data points correspond to daily forecasts with lead times 6, 12, 18 and 24 hours that are area-averaged over Central Africa (20°S–20°N, 20°W–30°E); missing data are blanked.

The Ensemble Prediction System

The characteristics of perturbation growth in the EPS were significantly changed due to the convection and vertical diffusion changes in Cy32r3. In a statistically consistent ensemble, the RMS error of the ensemble mean (computed over a sufficiently large sample) should match the ensemble standard deviation (*Palmer et al.,* 2006). For Cy32r2, the ensemble spread and the ensemble mean RMS error agree well from about day 5 onwards (Figure 9(a)). However, the good agreement from day 5 can only be achieved by using a large initial perturbation amplitude which results in an over-dispersive ensemble during the earlier forecast ranges.

Initial experimentation with the new convection and diffusion scheme indicated that the physics changes results in a significant increase in the ensemble standard deviation. This offered the opportunity to reduce the initial perturbation amplitude in order to improve the agreement between spread and ensemble mean RMS error at all forecast ranges. First, a reduction of the initial perturbation amplitude by 20% was tested in a sample of 13 summer and 13 winter cases. Results indicated that a further reduction of the initial perturbation amplitude was required and it was decided to reduce the initial perturbation amplitude by 30% in Cy32r3.

The faster perturbation growth due to the convection and diffusion changes, together with the reduced initial perturbation amplitude, results in an improved overall agreement between ensemble spread and ensemble mean RMS error in Cy32r3 (Figure 9(b)). The EPS no longer suffers from an over-dispersion in the early forecast ranges. The EPS evaluation for Cy32r3 is based on nearly seven weeks of daily ensemble forecasts from June, August and September 2007. The improved match between ensemble spread and ensemble mean RMS error are statistically significant (see confidence intervals in Figure 9).

doi:10.21957/33vbh2pla1

The Ranked Probability Skill Score (RPSS) evaluates the mean squared error of the predicted probabilities. In terms of this score the probabilistic prediction of 850 hPa temperature is significantly better in Cy32r3 than its predecessor in both hemispheres and at all forecast ranges (Figure 10(b)). For 500 hPa geopotential, the impact of Cy32r3 is neutral in the northern hemisphere and positive in the southern hemisphere (Figure 10(a)). Note, that there is no simple relationship between the probabilistic skill and the deterministic skill of the ensemble mean. For instance, while the impact of Cy32r3 on the RPSS of 500 hPa geopotential in the northern hemisphere is neutral, Cy32r3 has a positive impact on the RMS error of the ensemble mean (again with more than 99% statistical significance). By the same token, the impact on the RMS error of the ensemble mean is neutral for 850 hPa temperature in the northern hemisphere while a statistically significant positive impact was noted for the RPSS.

In addition to the changes already mentioned, the tangent-linear and adjoint model in the singular vector computation targeted on tropical cyclones use the new moist physics package in Cy32r3. The new package has been used operationally in 4D-Var since Cy32r2. Preliminary experimentation over 27 summer cases with the new moist physics package in the EPS singular vector computations indicates an improved reliability of forecasts of tropical cyclone strike probability and neutral impact on ensemble spread and skill scores in the extra-tropics.

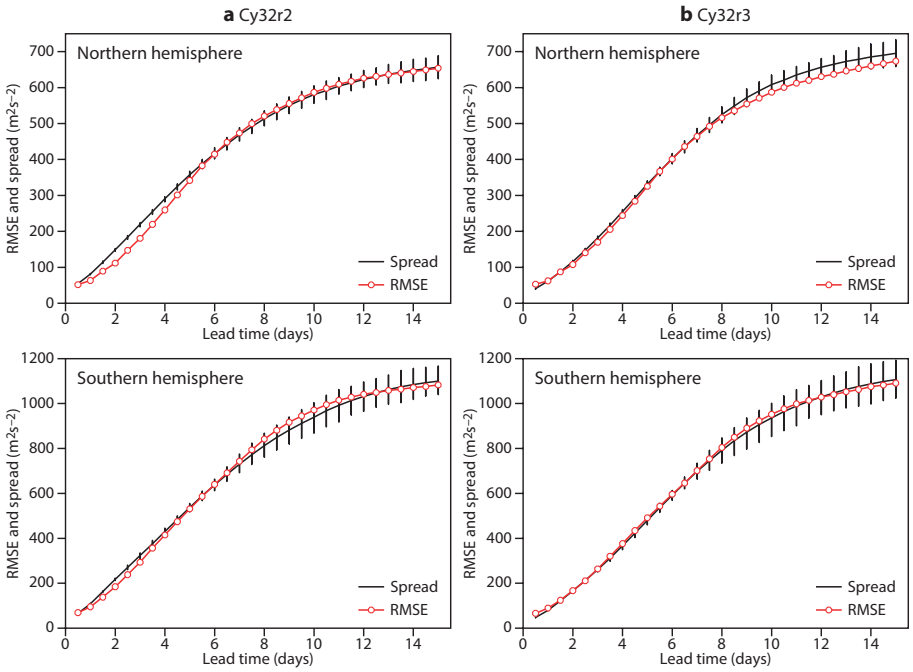

Figure 9 Ensemble standard deviation (spread) and ensemble mean RMS error (RMSE) as a function of forecast lead time for 500 hPa geopotential for the northern hemisphere (20°N–90°N, top panel) and southern hemisphere (20°S–90°S, bottom panel) for (a) Cy32r2 and (b) Cy32r3. Statistics are based on 69 cases during June to September 2007. The vertical bars are confidence intervals based on bootstrapping the dates in the sample of cases. If the spread falls within the bars, the ensemble is not significantly over- or under-dispersive (the probability of the spread being above or below the bar by chance is 1%).

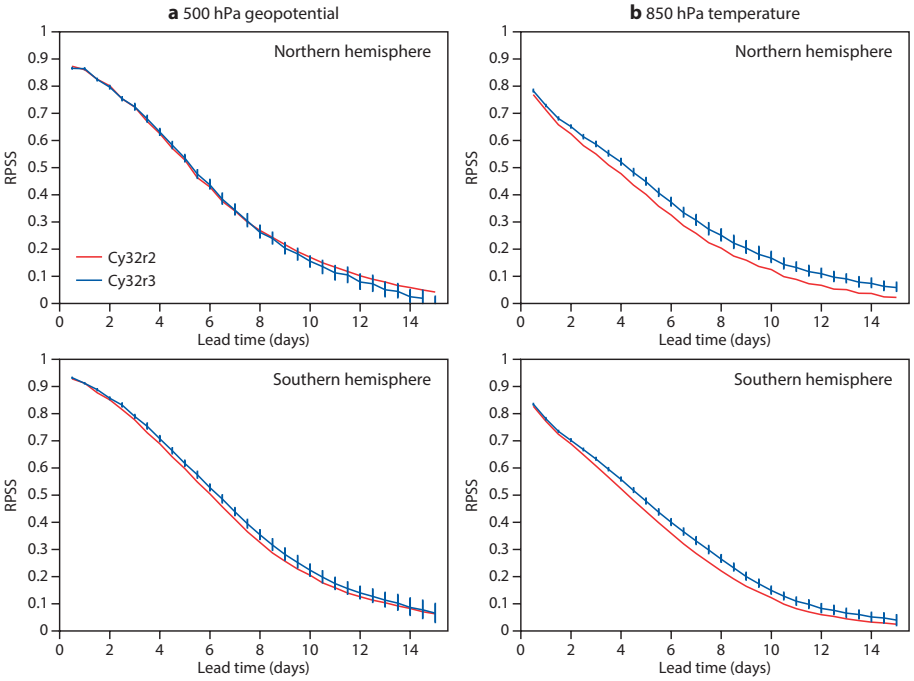

Figure 10 Ranked Probability Skill Score (RPSS) for Cy32r2 and Cy32r3 as a function of forecast lead time for the northern hemisphere (20°N–90°N, top panel) and southern hemisphere (20°S–90°S, bottom panel) for (a) 500 hPa geopotential and (b) 850 hPa temperature. The RPSS is determined for ten climatologically equally likely categories. Cy32r3 is significantly better (worse) than Cy32r2 at the 99% level if the red curve lies below (above) the vertical bars.

Monthly forecasts and the Madden-Julian Oscillation

The Madden-Julian Oscillation (MJO) is the dominant mode of intraseasonal predictability in the tropical atmosphere. Therefore, it is important that the monthly forecasting system accurately predicts its onset and evolution.

To assess the skill of the monthly forecasting system to predict an MJO event, 32-day coupled ocean-atmosphere integrations using a five-member ensemble have been performed for each day between 15 December 1992 and 31 January 1993 (46 ensemble integrations); this period corresponds to the Intense Observing Period (IOP) of TOGA-COARE. The MJO is diagnosed in these integrations using a method based on the technique of *Wheeler & Hendon* (2004). Combined Empirical Orthogonal Functions (EOFs) of OLR, 200 hPa velocity potential and 850 zonal wind averaged over 10°N–10°S are calculated using ECMWF operational data between 2002 and 2004. The EOF analysis is performed on the anomalies relative to the seasonally evolving climatology. The first two EOFs, which represent 18% and 17% of the variance respectively, describe variations associated with the MJO. Observations and forecasts are then projected onto these two EOFs. Different cycles from Cy28r3 onward (operational implementation 29 April 2004) have been run for the control period in order to assess the impact of changes in the physics on the skill of the monthly forecast system to predict an MJO event.

Figure 11 shows the amplitude of Principal Component 1 (PC1) averaged over the 46 integrations and the five members of the ensemble as a function of the forecast time. Results are similar for Principal Component 2 (PC2). Before Cy32r3, all versions of the IFS shared the same problem, namely a rapid drop in the amplitude of PC1 and PC2; the drop in the amplitude of the MJO can be seen in Figure 11. For instance, with Cy28r3 the MJO loses 25% of its amplitude after only five days of integrations, about 33% by day 10, and about 50% by day 20. This means that the impact of the MJO on the extra-tropics was likely to be strongly underestimated in those cycles. On the other hand Figure 11 shows that Cy32r3 is the first IFS cycle able to sustain the amplitude over the whole period of the integration. This is an important result since it implies that, for the first time, the monthly forecasting system may now be able to adequately represent the impact of the MJO on the extra-tropics.

Figure 12 illustrates the progress made in the representation of the MJO with the IFS. In Cy28r3 the OLR anomalies are very weak by day 15. Each new cycle increases the amplitude of the OLR anomalies (results are similar for velocity potential at 200 hPa and zonal wind at 850 hPa), and with Cy32r3 the OLR anomalies by day 15 are as intense as in ERA-40. However, the propagation of the MJO with Cy32r3 is slower than

 doi:10.21957/33vbh2pla1

in the analysis. In particular, the model has some difficulty propagating the convection from the Indian Ocean to the Pacific, and instead tends to maintain the convection over the Indian Ocean for too long. This deficiency may be related to an overestimation of convective precipitation over the maritime continent.

Concluding remarks

Apart from overall satisfactory forecast scores, the most positive outcome of implementing Cy32r3 is that it is possible to reasonably represent the atmospheric variability on a wide variety of time and space scales using a conventional set of physical parametrizations, without necessarily having to specifically use an explicit global representation of convection (as has been discussed in recent forums). This might come as a surprise, but considering that the modes discussed here are also eigenmodes of the (dry) atmosphere (*Wedi & Smolarkiewicz,* 2007), it seems reasonable to assume that it should be possible to develop a set of physical parametrizations that in some optimal way supports these modes. Furthermore, the results confirm that a good representation of variability comes with a good representation of the mean state.

If anything, the level of model activity in Cy32r3 is slightly overestimated. No attempt was made here to break this down into convection and diffusion components, but it seems to be related to some overestimation of mid-tropospheric moisture (in contrast to a too dry mid-troposphere in previous cycles), and possibly to an increase in wind shear near the trade wind inversion. However, the IFS is still unable to properly represent the stratospheric wind variability associated with the QBO, but current developments indicate that this can be achieved with a scheme that parametrizes the non-orographic gravity wave drag. Finally, there is development of an upgrade of the simplified linear set of physical parametrizations for the assimilation that closely matches the results of the non-linear schemes in Cy32r3. Some further impact on the analysis and the medium-range forecasts (in particular the humidity) in the tropics is expected from this development.

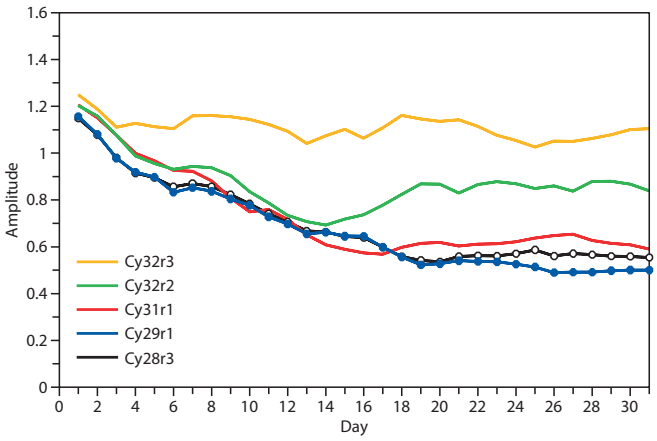

Figure 11 Amplitude of the first combined EOF of Outgoing Longwave Radiation (OLR), 200 hPa velocity potential and 850 hPa zonal wind as a function of forecast lead time from Cy28r3 to Cy32r3. The amplitude constitutes an average over each ensemble member and the 46 cases.

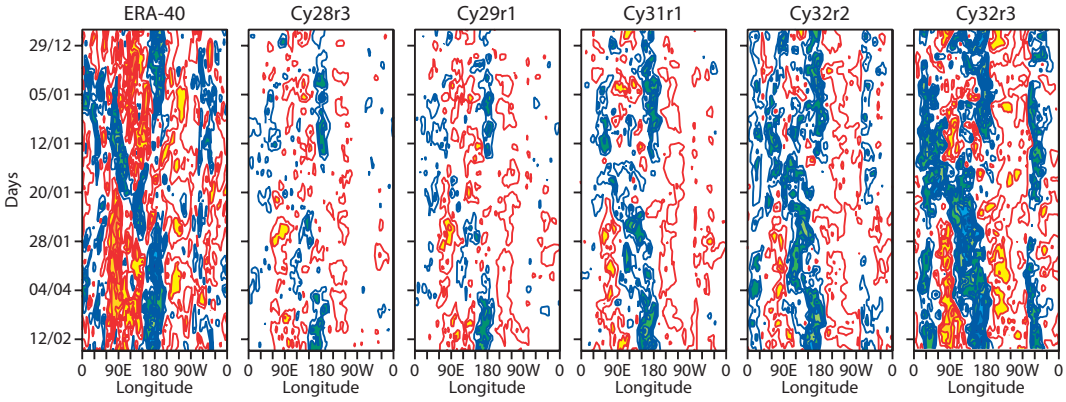

Figure 12 Hovmöller diagrams of the averaged Outgoing Longwave Radiation (OLR) between 10°S and 10°N from 29 December 1992 to 15 February 1993 as analysed by ERA-40 and obtained from forecasts with Cy28r3 to Cy32r3 using concatenated daily forecasts with a 15 day lead time. Red shading denotes warm OLR anomalies (negative phase of MJO), and blue shading cold anomalies (convectively active phase of MJO).

doi:10.21957/33vbh2pla1

Further Reading

Betts, A.K., J.H. Ball, P. Viterbo, A. Dai & **J.A. Marengo,** 2005: Hydrometeorology of the Amazon in ERA-40. *J. Hydrometeorol.,* **6,** 764–774. Also *ERA-40 Project Report 22*.

Gill, A.E., 1980: Some simple solutions for heat-induced tropical circulations. *Q. J. R. Meteorol. Soc.,* **106,** 447–462.

Morcrette, J.-J., H.W. Barker, M.J. Iacono, G. Mozdzynski, R. Pincus, D. Salmond & **S. Serrar,** 2007. A new radiation package McRAD. *ECMWF Newsletter No. 112,* 22–32.

Palmer, T., R. Buizza, R. Hagedorn, A. Lawrence, M. Leutbecher & **L. Smith,** 2006: Ensemble prediction: A pedagogical perspective. *ECMWF Newsletter No. 106,* 10–17.

Wedi, N.P. & **P.K. Smolarkiewicz,** 2007. A reduced model of the Madden-Julian oscillation. *Int. J. Numer. Meth. Fluids,* published online DOI:10.1002/fld.1612.

Wheeler, M.C. & **H.H. Hendon,** 2004: An all-season real-time multivariate MJO index: Development of an index for monitoring and prediction. *Mon. Wea. Rev.,* **132,** 1917–1932.

© Copyright 2016

European Centre for Medium-Range Weather Forecasts, Shinfield Park, Reading, RG2 9AX, England

The content of this Newsletter article is available for use under a Creative Commons Attribution-Non-Commercial-No-Derivatives-4.0-Unported Licence. See the terms at https://creativecommons.org/licenses/by-nc-nd/4.0/.

The information within this publication is given in good faith and considered to be true, but ECMWF accepts no liability for error or omission or for loss or damage arising from its use.

 doi:10.21957/33vbh2pla1